Binding of CO, NO, and O_2 to Heme by Density Functional and Multireference ab Initio Calculations

Mariusz Radoń*

Faculty of Chemistry, Jagiellonian University, ul. Ingardena 3, 30-060 Kraków, Poland

Kristine Pierloot

Department of Chemistry, University of Leuven, Celestijnenlaan 200F, B-3001 Heverlee-Leuven, Belgium

Received: July 9, 2008; Revised Manuscript Received: September 5, 2008

Using the CASSCF/CASPT2 approach, along with several DFT methods (PBE0, B3LYP, BP86, OLYP), we have investigated the bonding of CO, NO, and O_2 molecules to two model heme systems: an iron(II) porphyrin with and without an axial imidazole ligand. The experimentally available binding energies are best reproduced by the CASPT2 method and with the OLYP functional. The other functionals considered perform much worse, either severly overbinding (BP86) or underbinding (B3LYP, PBE0). Significant discrepancies between the different density functionals are observed, not only for the energetics but sometimes also for structure predictions. This confirms our viewpoint that a balanced treatment of the electronic exchange and correlation is vital to describe the weak metal−ligand bond between heme and CO, NO, or O_2. The binding energies ΔE_b were split into two contributions: the so-called spin-pairing energy ΔE_{sp} and the "inherent" binding energy ΔE_{b0}, and both contributions were analyzed in terms of method and basis set effects. We have also investigated the spin density distributions resulting from the bonding of the NO molecule (a noninnocent ligand) to heme. Our analysis at the DFT and CASSCF level shows that, while various density functionals predict qualitatively very different spin distributions, the CASSCF spin populations most closely correspond to the results obtained with the pure BP86 or OLYP rather than with the hybrid functionals.

1. Introduction

Binding energies of O_2, CO, and NO to heme sites of enzymes like myoglobin or hemoglobin are crucial for the activity of these diatomic molecules in respiration and regulation processes. As all three molecules have a similar size and polarity, they are discriminated mainly by a different affinity to the ferrous center.[1] It is thus very important and challenging to reliably reproduce their binding energies (especially the relative values) by quantum-chemical calculations. Apart from a better understanding of this particular problem, the accuracy of such calculations might serve as a real-world benchmark for the modeling of similar processes in the field of biocatalysis.

Several theoretical studies,[1−11] primarily based on Density Functional Theory (DFT), have provided insight into the geometries, electronic structures, and binding energies for the heme−XO complexes (in this paper the XO abbreviation is used for any of the three considered diatomic molecules). However, none of the theoretically computed binding energies satisfactorily reproduce the experimentally available affinities.[1,12,13] Particularly large errors are obtained for heme−NO complexes, which are severely underbound by hybrid density functionals.[1,10] On the other hand, nonhybrid functionals tend to overbind all three ligands. Due to the limited number of ab initio calculations available for similar systems, it is not clear whether the observed discrepancies with experiment should be attributed to deficiencies of the theoretical models (e.g., not considering the distal groups in the enzyme) or rather to inaccuracies of the DFT methodology itself.

There are basically two reasons why an accurate prediction of heme−XO binding energy might be difficult, particularly for DFT. First, the spin state of the iron changes during the XO addition, while spin state relative energies for transition metal complexes are known to require a high-level description of the electronic exchange and correlation.[14,15] Second, the energy of a covalent metal−ligand bond contains an important fraction of nondynamic correlation.[16,17] Additional complications occur for the complexes with O_2, suffering from a strong spin contamination in unrestricted single-determinant calculations.

In the present paper we investigate heme−XO binding using the Complete Active Space Self-Consistent Field/Second-Order Perturbation Theory (CASSCF/CASPT2) approach.[18,19] This multireference method is capable of reproducing spin state relative energies for a variety of ferrous complexes[14,15] as well as properly describing nondynamic correlation effects connected to metal−ligand bonds.[16,17] CASPT2 binding energies are calculated here for all three XO ligands, and compared to the DFT results obtained from both hybrid and nonhybrid functionals, as well as to the available experimental data. Prior to the calculations of the binding energies, we shortly discuss the spin state energetics of the free heme. We also give special attention to the electronic structure of the particularly interesting complexes with NO ($\{FeNO\}^7$ species[20]), analyzing its spin density distribution at both the CASSCF/CASPT2 and DFT levels.

The present study focuses on the quantum chemical description of heme−ligand interactions. Because the ab initio CASPT2 method is in use, the heme model must be necessarily kept rather simple. In particular, it lacks the distal residues present in the real enzyme, which are known to affect the binding energies.[12] Therefore, their influence on the binding energies—called herein as "the protein effect"—is estimated based on other theoretical

10.1021/jp806075b CCC: $40.75
Published on Web 10/23/2008

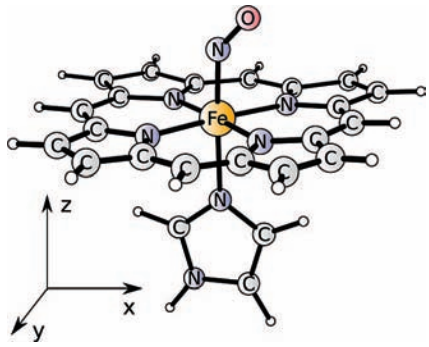

Figure 1. The model of the heme−ligand complex used in this study on the example of FeP(Im)(NO).

and experimental studies,[1,4,6,12,13] and taken into consideration when comparing our results to the experimental data of myoglobin.

2. Computational Details

2.1. Model. The model employed in the present study is limited to the ligands directly coordinated to the central iron. The heme group is modeled either as a porphyrin ring without substituents, denoted as P, or as a porphyrin with an axially coordinated imidazole ring, denoted as P(Im). Bonding of XO then gives the heme−XO complexes denoted as either FeP(XO) or FeP(Im)(XO). Note that similar models have been used in many previous studies.[1−3,10] The example model system is illustrated in Figure 1. All model systems have C_s symmetry (the xz plane being the symmetry plane) or higher: C_{4v} for FeP(CO), D_{4h} for FeP (except for the Jahn−Teller distorted ^3E_g states, for which the lower D_{2h} symmetry was used). The proper symmetry group was employed in all calculations, including the geometry optimization step.

2.2. Calculation of Binding Energies. Binding energies are given with respect to the lowest state with the spin multiplicity observed experimentally for the reactants and products: triplet for FeP,[21−24] quintet for FeP(Im),[25−30] singlet for the complexes with CO and O_2,[10,11] and doublet for the complexes with NO.[31,32] Counterpoise corrections for basis set superposition errors (BSSE) as well as an estimation of zero-point vibrational energies (ZPVE) are included in all calculated binding energies. All calculated data for these corrections may be found in the Supporting Information.

Since the spin state is changed upon ligand binding—from high or intermediate spin to low spin—we also investigate the binding energy with respect to the low-spin (singlet) state of FeP or FeP(Im), denoted ΔE_{b0}. The relation between the binding energy with respect either to the ground state (ΔE_b) or to the singlet state is given by

$$\Delta E_b = \Delta E_{b0} - \Delta E_{sp} \quad (1)$$

where ΔE_{sp} is so-called spin-pairing energy for the respective heme (i.e., the energy difference between the low spin and the ground state).

2.3. DFT Calculations. All DFT calculations were performed with the Turbomole 5.9[33] and Gaussian03[34] packages. Geometries were optimized at the DFT level with several functionals (PBE0,[35] B3LYP[36] (VWN III), BP86,[37,38] OLYP)[39,40] making use of the two basis sets defined in Table 1. Frequency calculations to estimate ZPVE corrections were performed at DFT level with the smaller basis set A. As the ZPVE corrections are similar for different functionals (see Supporting Information) the values from the BP86 functional were used instead of the OLYP ones (which were not computed). During the OLYP optimization of the FeP(Im)(NO) complex, the Fe−(Im) bond was unexpectedly broken. Therefore, to make all calculations consistent, the OLYP energies are in this case given for the BP86/A structures. (Except for this case, similar OLYP results were always obtained for both choices of structures.)

TABLE 1: Basis Sets Employed in DFT Calculations

basis set	definition
A	Fe: ecp-10-mdf[41] augmented with two f primitives (of 2.5 and 1.4 exponents); ligands: 6-31G(d)[42,43]
B	Fe: QZVPP;[44] ligands: TZVPP[45]

Open-shell cases were treated by means of the spin-unrestricted DFT formalism. For heme−O_2, the calculations converged to a broken symmetry (BS) solution, exhibiting antiferromagnetic coupling between the spin densities on the iron and on the ligand. As the BS wave function suffers from spin contamination, the obtained energy is a weighted average of the energy of the target state and the states of higher multiplicity. To approximately correct for this, a standard spin projection technique[46,47] was applied. It introduces an auxiliary high-spin (HS) state in which (by definition) all the orbitals being coupled for the BS state are filled with spin-up electrons. The correction to the energy of the BS state takes the form

$$\Delta E_J = xJ \quad (2)$$

where x is measure of spin contamination in the BS state

$$x = \langle S^2 \rangle_{BS} - S(S+1) \quad (3)$$

(S being half the difference in number of spin-up minus spin-down electrons), while J is the effective exchange coupling constant of the Heisenberg−Dirac−Van Vleck Hamiltonian[47−49]

$$J = \frac{E_{BS} - E_{HS}}{\langle S^2 \rangle_{HS} - \langle S^2 \rangle_{BS}} \quad (4)$$

The HS state is obtained from a separate energy calculation at the equilibrium geometry of the BS state. To construct the HS state, effective spins must be assigned to iron and to the ligand, which is possible upon inspection of the spin populations and the natural orbitals for the BS state (see Results for information about the electronic structure). For the O_2 complexes, coupling of one electron on iron with one electron on O_2 was found ((1,1) coupling), except for several cases where oxygen is bound very weakly and coupling of two electrons on iron with two electrons on O_2 ((2,2) coupling) is observed instead. Thus, the HS state either has triplet ((1,1) coupling) or quintet ((2,2) coupling) spin multiplicity. More information on the spin projection procedure can be found in the Supporting Information.

2.4. CASPT2 Calculations. CASSCF/CASPT2 calculations were performed with the Molcas package,[50,51] employing a Cholesky decomposition scheme for the two-electron integrals.[52] Structures from the PBE0/A calculations were used in these calculations, except for the O_2 complexes for which the BP86/A structures were chosen instead. This was done because the PBE0 functional hardly predicts any oxygen binding, giving structures which are presumably wrong (too long Fe−O distance); see Supporting Information. For these cases the structures from the nonhybrid functionals seem more correct. In all other cases the choice between BP86 and PBE0 structures does not change the CASPT2 results to a significant extent.

Two basis sets (denoted I and II) composed of atomic natural orbitals (ANO) were used in the CASPT2 calculations (Table 2). All core electrons (not Fe 3s,3p) were kept frozen during

TABLE 2: Basis Sets Employed in the CASPT2 Calculations

basis set	definition
I	Fe: ANO-RCC[53] 7s6p5d2f1g ligands: ANO-S[54] (N, O: 4s3p1d; C: 3s2p1d; H: 2s)
II	ANO-RCC[53] (Fe: 7s6p5d3f2g1h; N, O: 4s3p2d1f; C: 4s3p1d; H: 3s1p)

the CASPT2 calculations The calculations were performed using the IPEA-shifted zeroth-order Hamiltonian[55] (default in Molcas) with an imaginary level shift (0.1 hartree). Scalar relativistic effects were included in the calculations via the second-order Douglas−Kroll−Hess transformation.[56]

For FeP, the active space was constructed by distributing 8 electrons in 11 orbitals: five orbitals with predominant iron 3d character, a second 3d′ shell describing the *double-shell* correlation effect within the 3d shell, and the bonding Pσ−Fe $3d_{xy}$ combination, involved in nondynamic correlation effects associated with the occurrence of a covalent Fe−Pσ interaction.[16,17] For FeP(Im) the (8 in 11) active space was further extended with Imσ, thus giving a (10 in 12) space. These active spaces were used for the calculation of the different spin states in both complexes (Table 3), thus providing a balanced description of the spin pairing energy ΔE_{sp}. We note that all CASPT2 results in Table 3 include a correction term for the difference in ZPVE of the different spin states. This correction was taken from the DFT (frequency) calculation providing the structure for the CASPT2 calculation.

In FeP(XO) and FeP(Im)(XO), covalent iron−XO interactions give rise to additional strong correlation effects, which may be accounted for by extending the active space with the appropriate XO valence orbitals: σ, π, and π*. Including all five XO orbitals would lead to an active space of 16 or 17 orbitals, giving rise to computationally very demanding CASPT2 calculations. However, when employing this active space, we also experienced several practical problems already during the CASSCF step, in that orbitals with occupation numbers close to either 2 or 0 tended to rotate out of the active space in favor of respectively Fe 3s,3p core orbitals or antibonding ligand-centered orbitals. After an extensive series of test calculations were performed (the results of which may be found in the Supporting Information), the following active spaces were chosen for the calculation of the low-spin ground state in the respective FeP(XO) and FeP(Im)(XO) complexes. First, since in the low-spin ground state of all three complexes the occupation of the $3d_{xy}$ orbital is always small, the corresponding $4d_{xy}$ was removed from the active space. For XO = CO, $3d_{z^2}$ also remains unoccupied, such that $4d_{z^2}$ is also not necessary. All five CO orbitals were then included, thus giving an active space of (14 in 14) for FeP(CO) and (16 in 15) for FeP(Im)CO. For NO and O_2, XO σ-donation becomes less important and the corresponding XO σ orbital could be kept inactive. On the other hand, since in the NO and O_2 complexes the $3d_{z^2}$ orbital is always at least partially occupied, $4d_{z^2}$ should preferably be included in the active space. This was done for FeP(NO) and FeP(O_2), giving an active space of respectively (13 in 14) and (14 in 14) for these complexes. For FeP(Im)(NO) and FeP(Im)(O_2), including on top of this also Im σ turned out to be unfeasible. The effect of $4d_{z^2}$ on the binding energy ΔE_{b0} was therefore estimated from a separate calculation without Imσ active (and $4d_{z^2}$ either active or virtual), and added to the result obtained from the (15 in 14), (16 in 14) calculation (Imσ active, $4d_{z^2}$ virtual) for respectively FeP(Im)(NO) and FeP(Im)(O_2). We note that comparable active spaces to the ones used in this work have been proposed in two recent studies on similar heme complexes.[11,57]

Binding energies ΔE_{b0} with respect to the singlet state in FeP and FeP(Im) were obtained by subtracting from the total energies of the complexes (i) the CASPT2 energy of XO, calculated with the same valence orbitals active as in the complex: σ, π, π* for CO, but only π, π* for NO and O_2; (ii) the CASPT2 energy of either FeP or FeP(Im) (singlet) with an active space containing only three or four 4d orbitals, corresponding to the doubly occupied $3d_{x^2-y^2}$, $3d_{xz}$, $3d_{yz}$ orbitals and possibly also $3d_{z^2}$. This gives a balanced description of ΔE_{b0}. However, it means that for the calculation of the binding energy ΔE_b slightly different active spaces are used for the two terms in eq 1. The difference is situated in the calculation of the low-spin state of FeP and FeP(Im), containing one or two more active orbitals for the ΔE_{sp} than for ΔE_{b0}. However, since the orbitals concerned, $4d_{xy}$, $4d_{z^2}$, correspond to (almost) empty 3d orbitals, their effect on the total energy of the singlet state is (as expected) small: at most 2 kcal/mol. This difference should be considered as a possible error in the CASPT2 results which, we believe, cannot be avoided. We finally note that the CASPT2 results for ΔE_b (Table 6) and ΔE_{b0} (Table 5) are corrected for ZPVE (taken from the DFT calculations providing the structures used in CASPT2) and for BSSE. The latter corrections are, as expected, considerably more important for the CASPT2 than for the DFT results (6 kcal/mol for basis A, 0.6 kcal/mol for basis B). With basis I, BSSE corrections ranging between 10 and 13 kcal/mol were obtained. Going to basis II significantly reduces the BSSE, to 7−9 kcal/mol (see also the Supporting Information).

2.5. Estimation of the "Protein Effect". The distal residues of myoglobin, not included in the present model, do affect binding energies—hence this "protein effect" must be somehow estimated if the experimental binding energies for myoglobin are to be compared with our theoretical calculations. In several experimental[12,13] and theoretical[1,4,6] studies, it was recognized that the main effect is the formation of a hydrogen bond between the distal histidine (His) and the bound O_2 (which has partial anionic character[3]). Thereby, the complex with O_2 reaches an extra stabilization in myoglobin.[12] Still, controversies exist about the size of this protein effect for the O_2 complexes: the theoretical calculations (either DFT or DFT/Molecular Mechanics) notoriously predict much higher value (between 8 and 10 kcal/mol extra stabilization)[1,4,6] than is actually observed experimentally (only 2.5−3.8 kcal/mol).[12,13] The discrepancy can be caused either by limitations of the theoretical calculations (e.g., too small models, not considering entropic effects properly) or by an error or misinterpretation in the experiments—certainly, we do not pretend to address this complex issue herein. Instead, we propose to estimate the protein effect on the O_2 binding as an average of the available theoretical and experimental results; i.e., we assume a value of ∼6 kcal/mol.

On the other hand, the protein effect for two other ligands is much smaller (and also easier to estimate): ∼−1 kcal/mol for CO (i.e., it binds 1 kcal/mol weaker to myoglobin than to our model) and ∼0 kcal/mol for NO (i.e., the protein effect is negligible).[1,12]

3. Results and Discussion

3.1. Spin State Energies for the Free Hemes. An important question preceding the calculation of any binding energy is to identify the ground state of all reactants. Furthermore, since bonding of XO is in the present case accompanied by a spin-flip on iron from high- or intermediate- to low-spin, an accurate description of the relative energy of the different spin states in

TABLE 3: Relative Energies (kcal/mol) of Spin States for Free Ironporphyrins (Given with Respect to the Lowest State with Experimental Spin Multiplicity)

		$S = 0$		$S = 1$		$S = 2$	
		A/I	B/II	A/I	B/II	A/I	B/II
FeP	PBE0	38.7	36.7	0	0	−4.6	−0.5
	B3LYP	34.5	34.5	0	0	1.9	4.4
	OLYP	36.3	36.0	0	0	1.4	6.3
	BP86	37.1	35.6	0	0	9.8	15.3
	CASPT2[a]	35.8	35.3	0	0	−8.8	−6.5
	CASPT2[b]	35.4	34.9	0	0	−8.9	−6.5
FeP(Im)	PBE0	23.0	16.6	9.8	5.4	0	0
	B3LYP	12.6	9.6	3.5	0.7	0	0
	OLYP	13.9	8.0	3.9	−0.3	0	0
	OLYP[b]	13.7	8.0	4.2	0.1	0	0
	BP86	−0.8	−8.7	−4.3	−9.5	0	0
	CASPT2[a]	18.5	16.3	12.0	9.9	0	0
	CASPT2[b]	18.2	15.9	12.5	10.3	0	0

[a] For PBE0/A structure. [b] For BP86/A structure.

TABLE 4: Mulliken Spin Populations for the O_2 Complexes from DFT Calculations

	Fe	O(1)	O(2)
	Five-Coordinated Complex		
PBE0/A	2.12	−0.97	−1.01
PBE0/B	2.07	−0.98	−1.00
B3LYP/A	2.05	−0.94	−0.99
B3LYP/B	2.08	−0.98	−1.00
BP86/A	1.13	−0.42	−0.65
BP86/B	0.80	−0.29	−0.50
OLYP/A	1.63	−0.65	−0.83
OLYP/B	1.21	−0.46	−0.68
	Six-Coordinated Complex		
PBE0/A	2.07	−0.97	−0.99
PBE0/B	1.25	−0.47	−0.72
B3LYP/A	1.29	−0.50	−0.72
B3LYP/B	1.17	−0.43	−0.69
BP86/A	0.94	−0.32	−0.56
BP86/B	0.76	−0.25	−0.47
OLYP/A	1.47	−0.59	−0.77
OLYP/B	1.13	−0.42	−0.64

TABLE 5: Binding Energies (kcal/mol) of the Heme−XO Complexes with Respect to the Low-Spin State of the Hemes (ΔE_{b0})

	CO		NO		O_2[a]	
	A/I	B/II	A/I	B/II	A/I	B/II
	Five-Coordinated Complexes					
PBE0	37.7	40.7	39.6	42.5	39.6 (38.5)	37.5 (37.3)
B3LYP	33.8	37.3	36.3	41.2	33.2 (31.7)	32.9 (32.7)
OLYP	47.7	52.7	58.3	64.8	43.9 (30.5)	43.6 (35.9)
BP86	58.1	62.2	69.5	73.7	50.6 (43.5)	51.7 (46.7)
CASPT2	47.2	51.3	63.3	67.0	41.6	44.8
	Six-Coordinated Complexes					
PBE0	22.0	24.3	17.6	19.5	13.6 (12.5)	15.8 (9.3)
B3LYP	17.1	19.6	14.0	16.9	11.5 (4.9)	13.4 (7.6)
OLYP	21.9	25.4	24.2	28.3	13.3 (2.2)	13.1 (6.2)
BP86	29.6	32.1	32.2	34.1	17.7 (12.5)	18.6 (14.3)
CASPT2	32.0	35.7	34.2	37.8	22.2	25.7

[a] Values corrected for spin contamination; uncorrected values given within parentheses.

the free heme systems is of crucial importance. With this in mind, the relative energies of the free heme systems in their lowest (closed-shell) singlet ($S = 0$), triplet ($S = 1$), and quintet ($S = 2$) states are summarized in Table 3.

In Table 3 relative energies are given with respect to the lowest state with spin multiplicity corresponding to experiment: triplet for FeP,[21−24] quintet for FeP(Im).[25−30] The energy of the closed-shell singlet state (first column of the table) then corresponds to the spin pairing energy ΔE_{sp} (cf. eq 1).

First, it is useful to look at the principal orbital configuration of the relevant states. (Unless stated otherwise, this discussion refers both to the CASSCF and to the DFT description.) For a plot of the orbitals with predominant iron 3d character in FeP, we refer to ref 17 (see Figure 4 therein). With the porphyrin nitrogens situated in between the *x*- and *y*-axes (Figure 1), the $3d_{xy}$ orbital is most strongly destabilized by Fe−N σ interactions, while the $3d_{x^2-y^2}$ orbital remains essentially nonbonding. In FeP(Im), $3d_{z^2}$ is further destabilized by σ interaction with the axial imidazole. As such, the ($S = 2$) state in Table 3 corresponds to the configuration $(d_{x^2-y^2})^2(d_{xz})^1(d_{yz})^1(d_{z^2})^1(d_{xy})^1$, the ($S = 0$) state to $(d_{x^2-y^2})^2(d_{xz})^2(d_{yz})^2$. Note, however, that for FeP the state included here is not the lowest singlet state, the latter being instead an open-shell singlet corresponding to the configuration $(d_{x^2-y^2})^2(d_{xz,\,yz})^2(d_{z^2})^2$.[58,59] On the other hand, the character of the ($S = 1$) state depends both on the complex and on the method used. For FeP(Im) all methods predict the lowest triplet to correspond to the configuration $(d_{x^2-y^2})^2(d_{xz,\,yz})^3(d_{z^2})^1$. The same configuration is also predicted for FeP by DFT with the pure functionals BP86 and OLYP. However, both hybrid functionals B3LYP, PBE0, and also CASPT2, instead find $(d_{x^2-y^2})^2(d_{xz,\,yz})^2(d_{z^2})^2$ as the main configuration of the lowest triplet state. We should note, however, that the energy difference between the two triplet states concerned is small in all cases (2 kcal/mol or less).[58]

As Table 3 indicates, different methods predict a different ground state (GS) spin multiplicity. For the FeP complex the pure BP86, OLYP functionals as well as B3LYP correctly identify the GS as being a triplet, while PBE0 and also CASPT2 instead (incorrectly) predict a quintet GS. For FeP(Im) the experimental quintet GS is correctly reproduced only with the PBE0 and B3LYP functionals, as well as by CASPT2. Both B3LYP and OLYP however predict the quintet and triplet states very close in energy. In contrast, the BP86 functional strongly overstabilizes the triplet state. Furthermore, with BP86 even the closed-shell singlet is found below the high-spin GS.

Conforming with previous theoretical studies,[2,17,60−62] the computed relative energies of the different spin states strongly depend on the method as well as on the size of the basis sets. Comparing different DFT functionals, we find that the pure BP86 functional quite strongly overstabilizes the intermediate- and low-spin with respect to the high-spin state, whereas for

the hybrid functionals the splittings are determined by the amount of HF exchange, PBE0 (25% HF) systematically favoring the quintet state more than B3LYP (20% HF). In a recent study of the spin state energetics of a variety of six-coordinate ferrous compounds,[15] we found both OLYP and CASPT2 to work very well for the description of the high-spin−low-spin splittings in these complexes, providing results which are close both to each other and to the available experimental data. We note that this is no longer the case here. In Table 3 the OLYP results for the singlet−quintet and triplet−quintet splittings differ by 8−13 kcal/mol from the corresponding CASPT2 results. Instead they are much closer to B3LYP in all cases. It is also obvious that, in case of FeP, CASPT2 overstabilizes the high-spin state by at least 6.5 kcal/mol. We note that this result in fact presents a considerable improvement with respect to previous CASPT2 studies (performed with smaller basis sets and active spaces),[17,60] reporting quintet−triplet splittings between −20 and −10 kcal/mol. In a forthcoming publication[58] we will show that, after even further extending the basis set and active space and including also spin−orbit coupling, the correct GS for FeP may be computed also by CASPT2.

It is important to note, however, that the sensitivity of the spin state energetics to the applied method and basis sets only holds for the relative energies of, respectively, the triplet and singlet states with respect to the quintet state. The singlet−triplet splittings themselves are much less affected. This can be seen most clearly from the results of ΔE_{sp} for FeP in the first column of Table 3: comparing the results obtained with comparable basis sets (either A/I or B/II) the energies of the singlet state in FeP differ by less than 2 kcal/mol, while the differences for the other states amount to 20 kcal/mol and more. Also basis set effects are much more limited for this state, up to 2 kcal/mol, than for the other states, 3−8 kcal/mol. Looking at the configurations given above, we may conclude that the large fluctuations of the relative energies with respect to the high-spin state in these complexes should at least partially be traced back to the description of the destabilization by the surrounding porphin ring of the antibonding orbital with predominant iron $3d_{xy}$ character. Any transition involving a depopulation of this orbital is strongly affected, whereas transitions between the other four 3d orbitals, even though involving a spin change, are much less sensitive to the method and basis sets used. This conclusion also has an important consequence for the description of the bonding of XO to either FeP or FeP(Im) in section 3.3, since it means that the ΔE_{sp} term appearing in the expression of the binding energy (eq 1) is considerably more method and basis set dependent for the six-coordinated FeP(Im)(XO) than for the five-coordinated FeP(XO) complexes.

3.2. Electronic Structure of the Complexes with O_2 and NO. As opposed to the high- or the intermediate-spin ground state of the free heme systems, the complexes with CO, NO, and O_2 ligands exhibit a low-spin ground state. The CO complexes are described by a closed-shell ground state corresponding to the ferrous low-spin d^6 configuration, the CO coordinated in a straight fashion by means of "traditional" σ -donation and π -backdonation. On the other hand, bonding of both NO and O occurs in a bend fashion, with angles ranging between 140 and 147° for NO and between 119 and 125° for O_2, and their ground-state electronic structure is accomplished by an at least partial electron transfer between the metal and the ligand: from iron to O_2, giving rise to the Fe(III)−O_2^- Weiss-type resonance structure,[65] or from NO to iron, giving an Fe(I)−NO^+ complex.

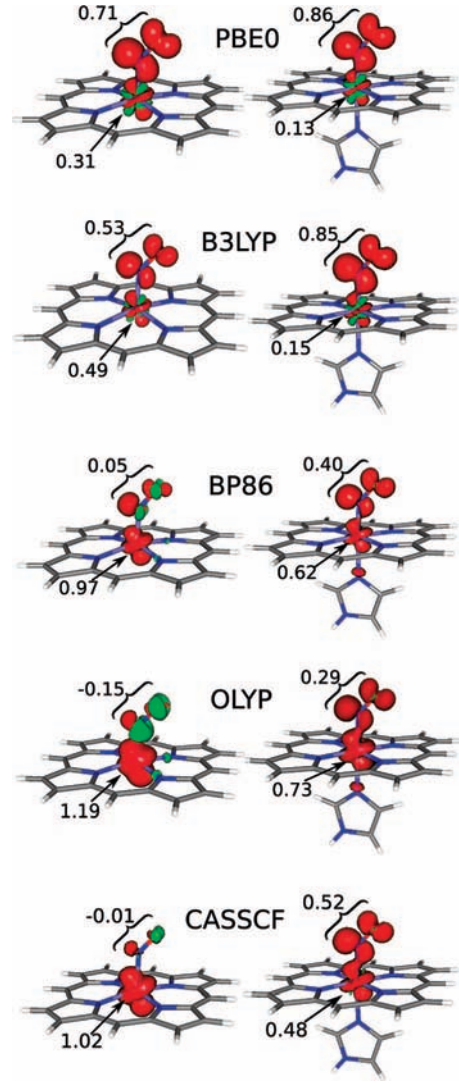

Figure 2. DFT and CASSCF spin densities for the doublet state of heme−NO complexes (basis A/I used, majority/minority spin density in red/green, contour value 5×10^{-3}, Mulliken spin populations given for Fe and NO).

The latter is illustrated by Figure 2, showing the spin densities in the FeP(NO) and FeP(Im)(NO) complexes, obtained from the different DFT functionals and with CASSCF. Bonding of the noninnocent NO ligand to the low-spin $3d^6$ Fe(II) results in a $^2A'$ ground state, both for the five- and six-coordinated complex,[31,32,63,64] the unpaired electron becoming delocalized over an iron 3d orbital with mixed $3d_{xz}-3d_{z^2}$ character and the π^* orbital of NO. As already noted previously,[63] the spin densities obtained from DFT strongly depend on the applied functional, in particular on the exchange part. Both hybrid functionals predict significantly more spin density on the NO moiety than the pure functionals. For the FeP(NO) complex both BP86 and OLYP in fact predict the unpaired electron to be localized predominantly on iron. (Actually, OLYP predicts a small amount of spin-down density on the NO antiferromagnetically coupled to spin-up density on the Fe.) In contrast, B3LYP almost equally divides the spin density between the NO and the Fe fragments, whereas PBE0 (with more exact exchange than B3LYP) pushes the spin density even more toward the NO. A similar dependence of the spin density on the applied density functional is observed for the six-coordinated complex. However, as compared to the five-coordinated complex, the spin density is always shifted toward the NO. Such a flow of spin

TABLE 6: Binding Energies [kcal/mol] for the Heme–XO Complexes (ΔE_b)

	CO		NO		O_2	
	A/I	B/II	A/I	B/II	A/I	B/II
Five-Coordinated Complexes						
PBE0	−1.0	4.0	0.9	5.8	0.9	0.8
B3LYP	−0.7	2.8	1.8	6.7	−1.3	−1.6
OLYP	11.4	16.7	22.0	28.8	7.6	7.5
BP86	21.0	26.5	32.4	38.1	13.4	16.1
CASPT2	11.4	16.0	27.5	31.7	6.2	9.9
exptl[66]			26.6[a]			
			28.9[b]			
Six-Coordinated Complexes						
PBE0	−1.0	7.7	−5.3	2.9	−9.4	−0.8
B3LYP	4.6	9.9	1.4	7.3	−1.0	3.8
OLYP	8.0	17.4	10.5	20.3	−0.5	5.1
BP86	30.4	40.6	33.0	42.7	18.5	27.4
CASPT2	13.5	19.4	15.8	21.6	4.1	9.9
exptl[1,12,13]	18.1[d]				12.3[c]	
	19.5[e]		22.8[e]		10.1[e]	

[a] Radiative association. [b] Associative equilibrium. [c] Dissociation barrier. [d] Estimated from *c* and relative CO/O_2 dissocation equilibrium constants. [e] Dissociation barriers for myoglobin, corrected for the absence of the protein environment (section 2.5).

density upon coordination of the sixth (imidazole) ligand is indeed also observed by magnetic circular dichroism (MCD) spectroscopy.[31,32]

Interestingly, the CASSCF spin densities show a qualitatively similar picture as obtained from the nonhybrid functionals (BP86, OLYP), both for the five- and six-coordinated complex: in FeP(NO) the unpaired electron is localized predominantly on Fe while NO carries only negligible spin density, thus pointing to a $Fe(I)-NO^+$ electronic structure. In the FeP(Im)(NO) complex approximately $^1/_2$ of the CASSCF spin density is localized on iron and the other $^1/_2$ on NO.

For the O_2 complexes, the DFT spin populations of the $^1A'$ ground state, given in Table 4, demonstrate the characteristic pattern of antiferromagnetic coupling between the Fe (excessive spin-up) and the O_2 (excessive spin-down).[2] The multideterminantal CASSCF wave function for the singlet produces zero spin density everywhere in space, which also results in zero spin populations. As such, interpretation in terms of antiferromagnetic coupling is more complicated than for DFT. From a previous analysis of the CASSCF wave function of $FeP(Im)(O_2)$ it was concluded[8] that the ground state of oxyheme is dominated by two configurations with approximately the same importance: the Weiss configuration, characterized by antiferromagnetic (1,1) coupling between between doublet Fe(III) and doublet O_2^-, and the Pauling configuration, i.e., a closed shell arising from interaction between singlet Fe(II) and singlet O_2. Other configurations appear in the wave function with significant weights, among which also the McClure configuration, built from (2,2) antiferromagnetic coupling between Fe(II) in the intermediate triplet spin and O_2 in its triplet ground state.

As can be seen from Table 4, and conform with earlier DFT studies,[2] the pure BP86 and OLYP functionals predict a partial charge transfer from Fe to the π^* orbitals of O_2, reducing the spin population of the O_2 moiety as compared to the free O_2 molecule (with two unpaired electrons), and ultimately leading to an antiferromagnetic Weiss-type electronic structure with approximately one spin-up electron on Fe(III) iron and one spin-down on the O_2^- moiety. (Note, however, that some of the spin populations are strongly basis set dependent, the larger basis set B always predicting the largest charge transfer.) With B3LYP, a different behavior is observed for the five- and six-coordinated complex. In $FeP(Im)(O_2)$, this functional predicts an oxygen spin population close to 1, similar to the pure functionals. However, for $FeP(O_2)$, the B3LYP oxygen spin population rather indicates *two* unpaired electrons, as it is for the free (unbound) oxygen molecule. A similar behavior is also found for the PBE0 functional. However, with this functional, only the largest basis set B gives a Weiss structure for the $FeP(Im)(O_2)$ complex, whereas $FeP(O_2)$ with both basis sets and $FeP(Im)(O_2)$ with basis A are predicted to have a (McClure) ground state arising from (2,2) antiferromagnetic coupling between triplet Fe(II) and O_2 in its triplet ground state.

The difference between both bonding types is also reflected in the structures of the oxygen complexes obtained with the different functionals. In those cases where a Weiss structure is found, charge transfer from iron into the O_2 antibonding π^* orbital results in an increased O−O bond length, by around 0.06 Å, as compared to free O_2. The Fe−O bond distance in these complexes is around 1.9 Å, typical for an Fe−O chemical bond. On the other hand, the PBE0 and B3LYP structures of $FeP(O_2)$ and the PBE0/A structure of $FeP(Im)(O_2)$ exhibit much larger Fe−O distances, around 2.5 Å, while the O−O distance in this case remains close to the free O_2 value (1.20−1.23 Å, depending on the functional). This indicates that in these complexes Fe−O bond formation is in fact very weak, an observation which is supported by the calculated binding energies, presented in the next section. For further details concerning the structures of the different complexes, we refer to the Supporting Information.

3.3. Binding Energies. The binding energies of CO, NO, and O_2 to FeP and FeP(Im) are presented in Tables 5 and 6. Table 5 gives the "intrinsic" binding energy ΔE_{b0}, with respect to the low-spin state of the proper heme, whereas in Table 6 the ΔE_{b0} numbers are combined (according to eq 1) with the corresponding spin pairing energies, ΔE_{sp} (Table 3), to give the final binding energy, ΔE_b, with respect to the lowest state corresponding to the experimental spin multiplicity. Note that all data in both tables include BSSE and ZPVE corrections. For the O_2 complexes, Table 5 gives the results for the binding energies both with and without (within parentheses) a correction for spin contamination (eq 2), whereas in Table 6 only the corrected results are included.

A few words must be said about the origin of the experimental results included in Table 6, as they rarely come from direct measuments. Two similar experimental binding energies are given for the five-coordinated complex with NO: from radiative association and associative equilibrium measurements.[66] Among the experimental results cited here, these two are presumably the most accurate and best suited for comparison with the computational results, as they are measured directly and for the gas phase. Table 6 also includes two sets of experimental data for the six-coordinated complexes. The first set refers to chelated protoheme (mono-3-(1-imidazoyl)-propylamide monomethyl ester) dissolved in an apolar medium, while the second set refers to myoglobin.[12] An estimation of the "protein effect" (see Computational Details) was subtracted from the myoglobin experimental data to give numbers comparable to the calculated results for the six-coordinated complexes. Furthermore, the data taken from myoglobin, as well as the experimental binding energy for the six-coordinated complex with O_2 in fact correspond to activation barriers for heme−XO dissociation, estimated from the dissociation rate constant[1,12] using transition state theory. This choice is motivated by the fact that entropy changes between the bound complex and the transition state for heme−XO dissociation may be expected to be minimal,

while the reverse association barrier should instead roughly correspond to the loss of entropy when binding the two fragments. The latter value may be expected to be the same for the three XO (an estimate of 10 kcal/mol is given in ref 1). Using dissociation barriers instead of the actual (free) energies of dissociation should therefore minimize "contamination" of the experimental data by entropy effects, which are not included in the calculated results. The value of 18.1 kcal/mol for the binding energy for the six-coordinated complex with CO was estimated from the relative values of the equilibrium constants for dissociation of CO and O_2. (The same cannot be done for NO since the equilibrium binding constant for this ligand was not recorded.) For a more thorough discussion of heme−XO dissociation energies and associated entropy effects, we refer to ref 1.

A first look at Tables 5 and 6 already shows that both the DFT and CASPT2 binding energies strongly depend on basis set size—the larger basis sets, expectedly, giving the strongest bonds (not always for O_2, which is a notable exception). The effect on ΔE_{b0} is limited to 5 kcal/mol or less in almost all cases. However, in ΔE_b this bond strengthening effect is combined with a considerable basis set effect on the spin pairing energy, in particular for FeP(Im) (Table 3), thus giving rise to basis set effects of up to 10 kcal/mol on, e.g., the BP86 binding energies of the FeP(Im)XO complexes. The rest of the discussion in this section will be based on the results obtained from the larger basis sets (B/II).

Looking first at the DFT results in Table 5, we note the following trends. Both for FeP and FeP(Im), the strongest Fe−XO bond is systematically predicted by BP86, followed by the other pure OLYP functional. Both hybrid functionals predict significantly smaller ΔE_{b0} values, in the order B3LYP < PBE0. Interestingly, as compared to the DFT results, CASPT2 predicts binding energies which are quite close (to within 3 kcal/mol) to OLYP for all three FeP(XO), whereas for the six-coordinated complexes the ΔE_{b0} values predicted by CASPT2 are significantly larger than any of the DFT results.

Going from Table 5 to Table 6 means substracting the spin pairing energy from ΔE_{b0}. Since for the five-coordinated complexes the values the ΔE_{sp} values (singlet−triplet splitting) are relatively indifferent to the method and basis set used (see also section 3.1), the ΔE_b values in Table 6 are quite uniformly lowered by 35−37 kcal/mol as compared to the corresponding data in Table 5. However, the trends observed between them are maintained, with BP86 giving the strongest bonds, both hybrid functionals giving very weak bonds, and both OLYP and CASPT2 in between and close to each other.

On the other hand, for the six-coordinated complexes, ΔE_{sp} stands for the singlet−quintet splitting in FeP(Im), showing a much more capricious behavior with respect to the computational method, thus jumbling up the relative values of the binding energies ΔE_b as compared to ΔE_{b0}. In particular, with BP86 strongly overstabilizing the singlet state and CASPT2 instead favoring the quintet state, the ordering of the binding energies obtained from both methods is reversed. As Table 6 shows, BP86 by far predicts the strongest Fe−XO bonds also for the six-coordinated complexes, whereas the CASPT2 values, as for FeP(XO), now again quite closely agree with OLYP. As for the hybrid functionals, with PBE0 more strongly favoring the quintet with respect to the singlet state than B3LYP, the former functional systematically predicts the weakest Fe−XO bond in the six-coordinated complexes.

As compared to the experimental data in Table 6, both hybrid functionals obviously grossly underestimate the strength of all three heme−XO bonds. On the other hand, the nonhybrid BP86 functional profoundly overbinds in all cases. Among the tested DFT methods, OLYP is the only functional predicting binding energies in a reasonable agreement with experiment. The largest error (5−7 kcal/mol) occurs for the six-coordinated O_2 complex. With the CASPT2 method and basis II, satisfactory results for ΔE_b are obtained in all cases. For FeP(NO), and presumably also for the other FeP(XO) complexes, the method overbinds by 2−5 kcal/mol. On the other hand, the results obtained for the six-coordinated complexes are very close, but systematically somewhat smaller (up to 1.1 kcal/mol) than the ΔE_b values deduced from experiment. This close agreement should, however, be put into some perspective, given that the high-to-low spin transition energy, which comes into these binding energies, is overestimated by CASPT2 (with the present basis sets) by at least a few kcal/mol. In the complete basis set limit, the present binding energies might increase by several kcal/mol, partly because of the very sensitive ΔE_{sp} term. It is also noteworthy that, for FeP(NO), the value of ΔE_b might be reduced by 6.5 kcal/mol (Table 3) to 25.2 kcal/mol, by calculating this property with respect to the (erroneous) CASPT2 quintet ground state rather than to the experimental triplet ground state of FeP, thus giving again slight underbinding. From this we believe that the accurate CASPT2 binding energies ΔE_b for the FeP(Im)(XO) complexes are the result of a cancelation of errors obtained from a method which inherently overbinds by a few kcal/mol.

It must be added here that for the myoglobin−CO complex yet another (smaller) binding energy was reported,[67] which would suggest a significantly smaller binding energy (11.9 kcal/mol) of FeP(Im)(CO). This result would imply that the CASPT2 binding energy for this complex could be overestimated and the B3LYP result could be more correct. (Similar suggestions that B3LYP works satisfactorily for CO binding were done on the basis of coupled clusters calculations for small model complexes.[10]) However, one must remember that the two different "experimental" binding energies for FeP(Im)(CO) were obtained from the experimental data in a different way. Sticking to the procedure outlined above (from the dissociation rate constant), one would obtain from ref 67 much higher binding energy (∼19 kcal/mol), similar to the previous values. Therefore, the apparent discrepancy of the experimental data could lie merely in their interpretation. At the moment, however, one must be aware that both binding energies for FeP(Im)(CO)—the higher ∼18−19 and the lower ∼12 kcal/mol—might be uncertain and this must not be forgotten when judging the accuracy of the theoretical methods.

Among the three studied diatomic molecules, O_2 is known to form the weakest bond to ferrous heme, while NO should form a stronger bond than CO. This trend is illustrated by the experimental binding energies of the six-coordinated complexes in Table 6. It is also reproduced by all calculated results for the five-coordinated complexes. However, for the six-coordinated complexes, both hybrid functionals fail to reproduce the correct relative affinity of NO as compared to CO. With B3LYP, CO binds more strongly by 2.6 kcal/mol than NO. With PBE0, the difference is even larger: 4.8 kcal/mol. The problem of too weak bonding of NO to ferrous heme was already noted in a previous B3LYP study,[1] where it was considered an important (worrying) issue for further investigation.

As mentioned, oxygen is found to give the weakest bond in all cases. However, the experimental binding energy to FeP(Im) may be satisfactorily reproduced only by the CASPT2 method. Except for BP86 which (as usually) overbinds, all DFT calculations produce a considerably too low binding energy.

This is particularly so for the hybrid functionals which, except for B3LYP in case of FeP(Im)(O_2), do not predict any O_2 bonding. For the five-coordinated complexes (and for the PBE0/A calculation on FeP(Im)(O_2)) the lack of O_2 bonding may be related to the calculated structural data and spin populations, discussed in the previous section. The very long Fe−O distances, as well as the oxygen O−O distances and spin populations close to free triplet O_2 (Table 4), were already indicative for the absence of any significant bonding. As can be seen from Table 5, the correction for spin contamination is also small (<1 kcal/mol) in all cases with (2,2) coupling, thus pointing to weak antiferromagnetic coupling. For the other, (1,1) coupling cases, the correction for spin contamination is obviously much larger, up to 7.7 kcal/mol (OLYP/B for FeP(O_2)). As a matter of fact, with the exception of BP86, all cases where DFT predicts a bonding heme−O_2 interaction it only does so after including the correction term. Thus, with this method any bonding of O_2 to ferrous heme is in fact completely determined by an approximate correction term. This (of course) strongly speaks in favor of the alternative CASPT2 method, which operates on the spin-pure wave function and does not need any correction to describe bonding in the O_2 complexes.

While this is the first study reporting CASPT2 binding energies for the complexes concerned, some of the DFT results reported here may be compared to previous calculations. For instance, in a previous B3LYP study of the six-coordinated complexes employing a similar model, the following binding energies were obtained: 16.9, 12.5, and 7.6 kcal/mol for binding of CO, NO, and O_2, respectively.[1] Although the same trends for the different XO ligands were found, these binding energies are systematically larger, by 4−7 kcal/mol, than the present results. The differences should be brought back to a combination of differences in the methodology, such as that in the previous study (a) imidazole was replaced by ammonia, (b) an apolar solvent was introduced by means of a continuum model, (c) ZPVE was not considered (an effect which reduces ΔE_b by around 3 kcal/mol, after accounting for the contributions to ΔE_{sp} and ΔE_{b0}; see the Supporting Information), (d) no correction for BSSE was included (an effect ranging in this study between 6.0 and 0.6 kcal/mol for either basis A or B). In a more recent DFT study,[10] binding energies of 18.1, 12.7, and −2.83 kcal/mol were obtained with B3LYP for the bonding of CO, NO, and O_2 to FeP(Im), respectively. No corrections for BSSE and ZPVE were included in these binding energies, and no correction for spin contamination was added for O_2. This may explain the larger values for ΔE_b for CO (by 8.2 kcal/mol) and NO (by 5.4 kcal/mol) as compared to this work, as well as the negative value for O_2. A third comparison is possible with previously published B86+P86 results.[2] This functional, though slightly different from BP86 (i.e., B88+P86), is expected to give similar binding energies. Indeed, our binding energies for the five-coordinated complexes are reasonably close to the previously published results: 26, 35, and 9 kcal/mol for CO, NO, and O_2 binding, respectively. Our binding energy for O_2 is larger, presumably because the cited result does not include any correction for spin contamination. To make an analogous comparison for the six-coordinated complexes, it is necessary to express our binding energies with respect to the triplet state of FeP(Im), since this state was used as a reference in the cited paper. When doing so, our BP86 binding energies become 31.3, 33.2, and 17.8 kcal/mol for CO, NO, and O_2 binding, respectively, which can be compared with 35, 36, and 15 kcal/mol taken from the cited paper. Again, given the small differences in methodology, both sets of binding energies essentialy agree.

4. Conclusions

The heme complexes with a series of inorganic diatomic ligands (CO, NO, and O_2) were theoretically investigated with several DFT methods (PBE0, B3LYP, OLYP, BP86) and the CASPT2 ab initio approach.

Ligand binding energies—the target properties of the present study—were computed with respect to the lowest state in the free heme with spin multiplicity reported by experiment, triplet for FeP but quintet for FeP(Im). A reasonably good agreement with experiment was found only for the CASPT2 and OLYP results. The performance of these two methods is especially satisfactory, given the very poor results of the other considered functionals, either strongly underbinding (the hybrid functionals), particularly for NO, or strongly overbinding (the BP86 functional). According to the present results, the OLYP functional is the only DFT method to be recommended for the energies of the similar systems. (Of course, we do not claim that this is a universal property of OLYP.) Its good energetic performance is, however, belittled by an apparent structural failure: OLYP does not predict a stable structure for the FeP(Im)(NO) complex. Moreover, it must be noted that all DFT binding energies for the O_2 complexes (including the OLYP one) strongly rely on an approximate correction term, included to deal with the spin contamination—without this term the quality of the result would be significantly worse. When judging the accuracy of the theoretical methods one must, however, be aware of possible errors in the experimental binding energies (e.g., for CO), as we discussed above.

The nitric oxide, as a so-called noninnocent ligand, significantly changes the electronic structure upon binding. This makes the spin distributions in the heme−NO complexes particularly interesting.[63] For the doublet state of FeP(NO) and FeP(Im)(NO), very different spin densities are obtained from different functionals, making the DFT results inconclusive. The CASSCF spin densities may therefore be used as a guide. We have found that the CASSCF spin densities are better reproduced by the pure functionals (BP86, OLYP) than by the hybrid ones.

In a previous computational study,[1] obtaining accurate binding energies for CO, NO, and O_2 to heme was described as being "more difficult than expected". Herein we also find this a very demanding task, in terms of basis set demands and electronic correlation effects. Certainly, the calculations performed in this work go well beyond routine quantum chemical modeling. However, despite some remaining doubts, we hope that a number of important aspects of heme−XO binding have been clarified by the present CASSCF/CASPT2 contribution, in comparison with DFT. It is expected that—along with software and hardware improvements—the CASSCF/CASPT2 methodology could become a more and more useful tool for energy prediction and solving the electronic structure of biochemical systems, in particular for electronically complicated situations, where DFT is no longer capable of providing quantitatively correct answers.

Acknowledgment. This investigation has been supported by grants from the Flemish Science Foundation (FWO), from the Concerted Research Action of the Flemish Government (GOA), and from the Polish State Committee for Scientific Research (KBN). The computational grants from The Academic Computer Center CYFRONET AGH are also acknowledged. Molecular graphics in Figure 1 was prepared with XYZViewer program obtained by courtesy of Sven de Marothy (Stockholm University).

Supporting Information Available: Tables of atomic coordinates, structural parameters, spin projection results, ΔE_{b0} values, ZPVE contributions, and BSSE corrections to binding energies and figures showing the iron displacement out of the porphyrin plane and contour plots of selected active orbitals. This material is available free of charge via the Internet at http://pubs.acs.org.

References and Notes

(1) Blomberg, L. M.; Blomberg, M. R.; Siegbahn, P. E. *J. Inorg. Biochem.* **2005**, *99*, 949–958.

(2) Rovira, C.; Kunc, K.; Hutter, J.; Ballone, P.; Parrinello, M. *J. Phys. Chem. A* **1997**, *101*, 8914–8925.

(3) Rovira, C.; Kunc, K.; Hutter, J.; Ballone, P.; Parrinello, M *Int. J. Quantum Chem.* **1998**, *69*, 31–35.

(4) Sigfridson, E.; Ryde, U. *J. Biol. Inorg. Chem.* **1999**, *4*, 99–110.

(5) Harvey, J. N. *J. Am. Chem. Soc.* **2000**, *122*, 12401–12402.

(6) Sigfridson, E.; Ryde, U. *J. Inorg. Biochem.* **2002**, *91*, 101–115.

(7) Jensen, K. P.; Roos, B.; Ryde, U. *J. Inorg. Biochem.* **2005**, *99*, 45–54.

(8) Jensen, K. P.; Roos, B.; Ryde, U. *J. Inorg. Biochem.* **2005**, *99*, 978.

(9) Rutkowska-Zbik, D.; Witko, M.; Stochel, G. *J. Comput. Chem.* **2007**, *28*, 825–831.

(10) Strickland, N.; Harvey, J. N. *J. Phys. Chem. B* **2007**, *111*, 841–852.

(11) Ribas-Ariño, J.; Novoa, J. J. *Chem. Commun.* **2007**, *2007*, 3160–3162.

(12) Olson, J. C.; Phillips, G. N. *J. Biol. Inorg. Chem.* **1997**, *2*, 544–552.

(13) Springer, B. A.; Egeberg, K. D.; Slighar, S. G.; Rohlfs, R. J.; Mathews, A. J.; Olson, J. C. *J. Biol. Chem.* **1989**, *264*, 3057–3060.

(14) Pierloot, K.; Vancoillie, S. *J. Chem. Phys.* **2006**, *125*, 124303.

(15) Pierloot, K.; Vancoillie, S. *J. Chem. Phys.* **2008**, *128*, 034104.

(16) Pierloot, K. Nondynamic Correlation Effects in Transition Metal Coordination Compounds. In *Computational Organometallic Chemistry*; Cundari, T. R. , Ed.; Marcel Dekker, Inc.: New York, 2001.

(17) Pierloot, K. *Mol. Phys.* **2003**, *101*, 2083–2094.

(18) Roos, B. O.; Taylor, P. R.; Siegbahn, P. E. M. *Chem. Phys.* **1980**, *48*, 157–173.

(19) Andersson, K.; Malmqvist, P.-Å.; Roos, B. O *J. Chem. Phys.* **1991**, *96*, 1218–1226.

(20) Westcott, B. L.; Enemark, J. L. Transition Metal Nitrosyls. In *Inorganic Electronic Structure and Spectroscopy*; Solomon, E. I., Lever, A. B. P. , Eds.; Wiley: New York, 1999; Vol. 2.

(21) Collman, J. P.; Hoard, J. L.; Kim, N.; Lang, G.; Reed, C. A. *J. Am. Chem. Soc.* **1975**, *97*, 2676–2681.

(22) Goff, H.; La Mar, G. N.; Reed, C. A. *J. Am. Chem. Soc.* **1977**, *99*, 3641–3646.

(23) Kitagawa, T.; Teraoka, J. *Chem. Phys. Lett.* **1979**, *63*, 443–446.

(24) Obara, S.; Kashiwagi, H. *J. Chem. Phys.* **1982**, *77*, 3155.

(25) Hu, C.; Roth, A.; Ellison, M.; An, J.; Ellis, C.; Schulz, C.; Scheidt, W. *J. Am. Chem. Soc.* **2005**, *127*, 5675–5688.

(26) Hu, C.; An, J.; Noll, B. C.; Schulz, C. E.; Scheidt, W. R. *Inorg. Chem.* **2006**, *45*, 4177–4185.

(27) Kent, T. A.; Spartalian, K.; Lang, G. *J. Chem. Phys.* **1979**, *71*, 4899–4908.

(28) Goff, H.; La Mar, G. N. *J. Am. Chem. Soc.* **1977**, *99*, 6599–6606.

(29) Momenteau, M.; Scheidt, W. R.; Eigenbrot, C. W.; Reed, C. A. *J. Am. Chem. Soc.* **1988**, *110*, 1207–1215.

(30) Ellison, M.; Schulz, C.; Scheidt, W. *Inorg. Chem.* **2002**, *41*, 2173–2181.

(31) Praneeth, V.; Neese, F.; Lehnert, N. *Inorg. Chem.* **2005**, *44*, 2570–2572.

(32) Praneeth, V.; Nather, C.; Peters, G.; Lehnert, N. *Inorg. Chem.* **2006**, *45*, 2795–2811.

(33) Ahlrichs, R.; Horn, H.; Schaefer, A. ; Treutler, O. ; Haeser, M.; Baer, M.; Boecker, S.; Deglmann, P.; Furche, F. *Turbomole v5.9*; Quantum Chemistry Group: Universitaet Karlsruhe, Germany.

(34) Frisch, M. J. ; Trucks, G. W.; Schlegel, H. B.; Scuseria, G. E.; Robb, M. A.; Cheeseman, J. R.; Montgomery, J. A., Jr.; Vreven, T.; Kudin, K. N.; Burant, J. C.; Millam, J. M.; Iyengar, S. S.; Tomasi, J.; Barone, V.; Mennucci, B.; Cossi, M.; Scalmani, G.; Rega, N.; Petersson, G. A.; Nakatsuji, H.; Hada, M.; Ehara, M.; Toyota, K.; Fukuda, R.; Hasegawa, J.; Ishida, M.; Nakajima, T.; Honda, Y.; Kitao, O.; Nakai, H.; Klene, M.; Li, X.; Knox, J. E.; Hratchian, H. P.; Cross, J. B.; Bakken, V.; Adamo, C.; Jaramillo, J.; Gomperts, R.; Stratmann, R. E.; Yazyev, O.; Austin, A. J.; Cammi, R.; Pomelli, C.; Ochterski, J. W.; Ayala, P. Y.; Morokuma, K.; Voth, G. A.; Salvador, P.; Dannenberg, J. J.; Zakrzewski, V. G.; Dapprich, S.; Daniels, A. D.; Strain, M. C.; Farkas, O.; Malick, D. K.; Rabuck, A. D.; Raghavachari, K.; Foresman, J. B.; Ortiz, J. V.; Cui, Q.; Baboul, A. G.; Clifford, S.; Cioslowski, J.; Stefanov, B. B.; Liu, G.; Liashenko, A.; Piskorz, P.; Komaromi, I.; Martin, R. L.; Fox, D. J.; Keith, T.; Al-Laham, M. A.; Peng, C. Y.; Nanayakkara, A.; Challacombe, M.; Gill, P. M. W.; Johnson, B.; Chen, W.; Wong, M. W.; Gonzalez, C.; Pople, J. A. *Gaussian 03, Revision C.02*; Gaussian, Inc.: Wallingford, CT, 2004.

(35) Perdew, J. P.; Ernzerhof, M.; Burke, K. *J. Chem. Phys.* **1996**, *105*, 9982–9985.

(36) Becke, A. D. *J. Chem. Phys.* **1993**, *98*, 5648–5652.

(37) Becke, A. D. *Phys. Rev. A* **1988**, *38*, 3098–3100.

(38) Perdew, J. P. *Phys. Rev. B* **1986**, *33*, 8822–8824.

(39) Handy, N. C.; Cohen, A. J. *Mol. Phys.* **2001**, *99*, 403–412.

(40) Lee, C.; Yang, W.; Parr, R. G. *Phys. Rev. B* **1988**, *37*, 785–789.

(41) Dolg, M.; Wedig, U.; Stoll, H.; Preuss, H. *J. Chem. Phys.* **1987**, *86*, 866–872.

(42) Hehre, W.; Ditchfield, R.; Pople, J. *J. Chem. Phys.* **1972**, *56*, 2257–2261.

(43) Francl, M.; Petro, W.; Hehre, W.; Binkley, J.; Gordon, M.; DeFrees, D.; Pople, J. *J. Chem. Phys.* **1982**, *77*, 3654–3665.

(44) Weigend, F.; Furche, F.; Ahlrichs, R. *J. Chem. Phys.* **2003**, *119*, 12753–12762.

(45) Weigend, F.; Häser, M.; Patzelt, H.; Ahlrichs, R. *Chem. Phys. Lett.* **1998**, *294*, 143–152.

(46) Siegbahn, P. E. M.; Blomberg, M. R. A. *Annu. Rev. Phys. Chem.* **1999**, *50*, 221–249.

(47) Soda, T.; Kitagawa, Y.; Onishi, T.; Takano, Y.; Shigeta, Y.; Nagao, H.; Yoshioka, Y.; Yamaguchi, K. *Chem. Phys. Lett.* **2000**, *319*, 223–230.

(48) Rodriguez, J.; Wheeler, D.; McCusker, J. *J. Am. Chem. Soc.* **1998**, *120*, 12051–12068.

(49) Rodriguez, J. H.; McCusker, J. K. *J. Chem. Phys.* **2002**, *116*, 6253–6270.

(50) Andersson, K.; Barysz, M.; Bernhardsson, A.; Blomberg, M.; Cooper, D. ; Fülscher, M.; de Graaf, C.; Hess, B.; Karlstrom, G.; R. Lindh, P.-Å. M.; Nakajima, T.; Neogrady, P.; Olsen, J.; Roos, B.; Schimmelpfennig, B. ; Schütz, M.; Seijo, L. ; L. Serrano-Andrés, P. E. M. Siegbahn, J. S.; Thorsteinsson, T.; Veryazov, V.; Widmark, P.-O. *MOLCAS, version 7.0*; Lund Univeristy: Sweden, 2007.

(51) Karlström, G.; Lindh, R.; Malmqvist, P.-Å.; Roos, B.; Ryde, U.; Veryazov, V.; Widmark, P.-O.; Cossi, M.; Schimmelpfennig, B.; Neogrady, P.; Seijo, L *Comput. Mater. Sci.* **2003**, *28*, 222–239.

(52) Aquilante, F.; Pedersen, T. B.; Lindh, R. *J. Chem. Phys.* **2007**, *126*, 194106.

(53) Roos, B. O.; Lindh, R.; Malmqvist, P.-Å.; Veryazov, V.; Widmark, P.-O *J. Phys. Chem. A* **2005**, *109*, 6575–6579.

(54) Pierloot, K.; Dumez, B.; Widmark, P.-O.; Roos, B *Theor. Chim. Acta* **1995**, *90*, 87–114.

(55) Ghigo, G.; Roos, B.; Malmqvist, P. -Å. *Chem. Phys. Lett.* **2004**, *396*, 142–149.

(56) Reiher, M.; Wolf, A. *J. Chem. Phys.* **2004**, *121*, 10945–10956.

(57) Jaworska, M. *Chem. Phys.* **2007**, *332*, 203–210.

(58) Pierloot, K.; Vancoillie, S.; Radoń, M. To be published.

(59) Blomberg, M. R.; Johansson, A. J.; Siegbahn, P. E. *Inorg. Chem.* **2007**, *46*, 7992–7997.

(60) Choe, Y.-K.; Nakajima, T.; Hirao, K.; Lindh, R. *J. Chem. Phys.* **1999**, *111*, 3837–3845.

(61) Liao, M.-S.; Watts, J.; Huang, M.-J. *J. Phys. Chem. A* **2007**, *111*, 5927–5935.

(62) Khvostichenko, D.; Choi, A.; Boulatov, R. *J. Phys. Chem. A* **2008**, *112*, 3700–3711.

(63) Ghosh, A. *J. Biol. Inorg. Chem.* **2006**, *11*, 712–724.

(64) Conradie, J.; Quarless, D.; Hsu, H.-F.; Harrop, T.; Lippard, S.; Koch, S.; Ghosh, A. *J. Am. Chem. Soc.* **2007**, *129*, 10446–10456.

(65) Silaghi-Dumitrescu, R.; Silaghi-Dumitrescu, I. *J. Inorg. Biochem.* **2006**, *100*, 161–166.

(66) Chen, O.; Groh, S.; Liechty, A.; Ridge, D. P. *J. Am. Chem. Soc.* **1999**, *121*, 11910–11911.

(67) Projahn, H.-D.; van Eldik, R. *Inorg. Chem.* **1991**, *30*, 3288–3293.

JP806075B